Morphological and Textural Analysis of Centroblasts in Low-Thickness Sliced Tissue Biopsies of Follicular Lymphoma

Emmanouil Michail, Kosmas Dimitropoulos, Triantafyllia Koletsa, Ioannis Kostopoulos and Nikos Grammalidis

Abstract— **This paper presents a new method for discriminating centroblast (CB) from non-centroblast cells in microscopic images acquired from tissue biopsies of follicular lymphoma. In the proposed method tissue sections are sliced at a low thickness level, around 1-1.5μm, which provides a more detailed depiction of the nuclei and other textural information of cells usually not distinguishable in thicker specimens, such as 4-5μm, that have been used in the past by other researchers. To identify CBs, a morphological and textural analysis is applied in order to extract various features related to their nuclei, nucleoli and cytoplasm. The generated feature vector is then used as input in a two-class SVM classifier with ε-Support Vector Regression and radial basis kernel function. Experimental results with an annotated dataset consisting of 300 images of centroblasts and non-centroblasts, derived from high-power field images of follicular lymphoma stained with Hematoxylin and Eosin, have shown the great potential of the proposed method with an average detection rate of 97.44%.**

I. Introduction

Follicular lymphoma (FL) is the second most common lymphoma diagnosed in the United States and Western Europe. It accounts for about 20% of all non-Hodgkin lymphomas and 70% of indolent lymphomas [1]. It mainly affects lymph nodes. When the affected lymph nodes are seen under the microscope, they show rounded structures called "follicles", which explains the term 'follicular'. The neoplastic cells consist of a mixture of centrocytes, which are small- to medium-sized cells and centroblasts (CBs), which are large cells.

The World Health Organization Classification has adopted grading from 1 to 3 based on the number of CBs counted per high power field (HPF), which is a microscopic image acquired at a magnification level of ×400 (the magnification of objective lens (×40) multiplied by the magnification of ocular lens (×10)): Grade I with 0-5 CBs/HPF, Grade II with 6-15 CBs/HPF and Grade III with more than 15 CBs/HPF [1]. CB count is performed manually by the pathologist using an optical microscope and Hematoxylin and Eosin (H&E) stained tissue sections. An average CB number is calculated over ten random HPFs. Manual histological grading of FL is a time consuming process and requires considerable effort and extensive training. Furthermore, since this method uses only ten HPFs for CB count, results for specimens with high tumor heterogeneity are vulnerable to sampling bias. This may lead to inappropriate clinical decisions on timing and type of therapy [2]. Hence, there is a need for a computer assisted method which will improve reproducibility and reliability of the grading process and will reduce the time needed for diagnosis.

Several studies have addressed the issue of classification between CB and non-CB cells in FL images. Classification is often based on morphological and topological features from the cell regions [3], texture features [2, 4], as well as graph-based features [5]. Principal Component Analysis (PCA) is often employed to identify the most discriminative features. In a recent study [6], the whole image of the cell with its surrounding is considered as a feature vector. In that way, all the features mentioned by the pathologists are being incorporated and redundant features are removed by linear and nonlinear dimensionality reduction methods.

However, most of the aforementioned studies have been conducted using FL tissue sections sliced at a thickness of around 4-5μm. Even though the most important features of the cells (size, shape, cytoplasm) are easily traceable at this level of thickness, it has been noticed that some other features, that also contribute to cell classification (like the number of nucleoli) need a lower thickness level in order to be detected. This is because thicker slices result in a less detailed depiction of the nuclei, the main cytological component. An illustration of the differences between thick-sliced (4μm) and thin-sliced FL (1μm) specimens can be seen in Fig. 1. CB in thin-sliced tissue section appears brighter and nucleoli are more distinguishable whereas, in thick-sliced tissue section CB appears darker and does not reveal too much information for the interior of the nucleus. As a consequence, it is probable that medical experts assessing these images, will rely mainly on nuclear size and shape, in order to distinguish between CB and non-CB cells. However, there are cases of large non-malignant cells (like dendritic cells, endothelial cells and osteocytes) that could be erroneously classified as CBs, if the interior of the nucleus is not carefully inspected during the classification of a cell. For example, Fig. 2 depicts two indicative images of endothelial and CB cells, both derived from 1μm tissue sections. From these images, it is obvious that size and shape features are not enough in order to classify these cells.

The research leading to these results has received funding from the European Union, Seventh Framework Programme (FP7/2007-2013) under grant agreement n° 247091.

E. Michail, K. Dimitropoulos and N. Grammalidis are with the Information Technologies Institute, Centre for Research and Technology Hellas, Thessaloniki, Greece, 57001 (PO Box 60361) (+302310464160; fax: +302310464164; e-mail: michem@iti.gr).

T. Koletsa and I. Kostopoulos are with Pathology Department, Medical School, Aristotle University of Thessaloniki, Thessaloniki, Greece, 54124 (e-mail: koletsa@med.auth.gr).

This paper describes a novel method for the classification of CBs in FL images, obtained from 1 to 1.5μm thick tissue sections. Towards this end, a combination of morphological and textural features is proposed, exploiting so the aforementioned advantages of thin-sliced specimens. More specifically, various features related to the nuclei, nucleoli and cytoplasm of the cells are employed for the modeling of CB cells. The generated feature vector is then used as input in a two-class SVM classifier with ε-Support Vector Regression and radial basis kernel function. To evaluate the proposed method an annotated database, containing 120 CB images and 180 non-CB images, was created (CERTH/AUTH database) [7], while experimental results with different classifiers are presented in the paper.

(a) (b)

Figure 1. *Images of centroblasts derived from HPF images generated using slice thickness of a) 4μm and b) 1μm.*

(a) (b)

Figure 2. *a) Cell annotated as endothelial by the pathologists and b) cell annotated as CB.*

II. Methodology

To discriminate between malignant and non-malignant cells[1], textural and morphological characteristics are extracted from the cells. The combination of the classification features proposed here has been formed according to the guidelines of medical experts and statistical tests. Specifically, ten different features are being extracted, which are described in detail in the following subsections.

A. Morphological analysis of nucleus

Two of the most basic characteristics of nuclei are their size and shape. Specifically, CBs are large and usually round cells [8] whereas, most non-CB cells have small nuclei and some cases of large non-CBs have elongated shape [9]. The difference in size between CBs and small non-CBs can be observed in Fig. 3, where two representative cases of a CB and a small healthy cell are depicted. By applying connected component labeling, individual nuclei are identified and their size is being estimated, constituting the first feature. In order to assess the shape of the nucleus, the perimeter of the nucleus is extracted and the best fitting ellipse is estimated using the Orthogonal Distance Regression (ODR) algorithm [10]. Subsequently, two shape features are extracted: a) the aspect ratio (major to minor axis ratio) and b) the ellipse residual (average geometric distance between pixels of the perimeter and pixels of the ellipse).

(a) (b)

Figure 3. *A representative case of (a) a CB and (b) a small non-CB cell*

B. Textural analysis of nucleus

Several types of (mainly small) non-CBs have a relatively dark nucleus, contrary to the nuclei of CBs, which are usually bright, as it is shown in Fig. 3. Additionally, through comparison of the nuclear texture of some types of (mainly large) non-CB cells and CBs, it can be observed that CBs are characterized by a higher non uniformity than non-CBs (Fig. 4). In order to encapsulate this information, we used the intensity histogram of the nucleus and the Gray-Level Run Length (GLRL) algorithm [11].

Specifically, the grayscale histogram of the nucleus was calculated and the mean value and the skewness of the histogram were extracted. Additionally, GLRL algorithm was used, as described in [12], in order to calculate the Gray-Level Non-uniformity (GLN) of the nucleus, which is a quantitative measure of textural abnormalities.

(a) (b)

Figure 4. *A representative case of (a) a centroblast and (b) a dendritic cell both derived from the same HPF image.*

C. Nucleoli detection

CBs usually have more and larger nucleoli than healthy cells [8]. In order to calculate the number and size of nucleoli, the following nucleoli detection algorithm was developed, which is depicted in Fig. 5.

Since nucleoli are dark regions inside the nucleus, we initially applied intensity thresholding to filter out non-candidate regions (i.e. bright regions). Specifically, Expectation Maximization (EM) algorithm is used to estimate the number of different intensity zones (classes), by using the minimum description length (MDL) criterion [13]. Assuming that intensity values are modeled as a Gaussian mixture model, MDL works by attempting to find the model order which minimizes the number of bits that would be required to code both the input data samples (intensity values) and parameters of the Gaussian mixture. The darkest class corresponds to the nucleoli. A new image of the nucleus is generated by keeping only the pixels belonging to the darkest class, as shown in Fig. 5 (b).

Subsequently, Circular Hough Transform [14] is applied to this image in order to detect small dark circles

[1] In the rest of the paper nuclei are also referred to as "cells"

representing the nucleoli (Fig. 5 (c)). The radius range for the detection is empirically set to {2-5} pixels. Often, circle detection leads to false positives, where the circle encompasses not only dark circular areas but bright areas too (Fig. 5 (d)). In order to eliminate false detections, the interior of each circle is examined and, if a large amount of pixels (empirically set to 40%) does not belong to the darkest class, the circle is rejected. Pixels belonging both to the darkest class and the remaining circles are considered to constitute the nucleoli. After the detection of nucleoli, their number, total area and maximum area are calculated for each cell.

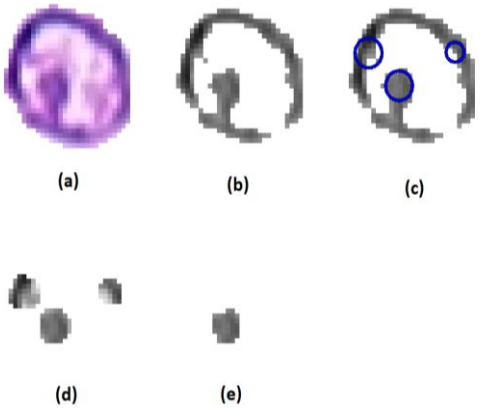

Figure 5. *Nucleoli detection on a CB. a) Initial RGB image of the nuclei, b) the darkest class of pixels after intensity MDL, c) circles are the result of Circular Hough Transform on the darkest class, d) the interior of the circles, e) pixels that belong to the intersection of the darkest class and the remaining circles, after discarding circles containing a large amount of bright components.*

It should be mentioned that small dark cells should be excluded from the aforementioned procedure since they can erroneously lead to the detection of large or many nucleoli. To this end, cells with size less than 2σ from the average size of CBs in the CERTH/AUTH database and with mean histogram value less than 2σ from the average histogram were filtered out.

D. Intensity histogram of the cytoplasm

According to [8], CBs usually have no sufficient cytoplasm and the exterior of the nuclei appears brighter than non-CB cells. In order to encapsulate this information the grayscale histogram of the surrounding area of the nucleus was calculated. In order to include only the proximate area of the nucleus, the initial mask of the candidate cell was kept and dilation was applied on it, with a disk-shaped structuring element of radius r=7. The pixels of the dilated mask that did not belong to the initial mask were considered as the proximate area of the nucleus. Among the first four histogram moments of the cytoplasm, histogram variance revealed the most statistically significant differences between CBs and non-CBs and consequently, it was included in the classification feature set.

E. Classification algorithms

After feature extraction, all features are being normalized by calculating the standard deviation of each feature and dividing all feature values by this standard deviation. In order to define the optimum classification scheme, five different classification algorithms were applied on the normalized data: classification tree [15], naive bayes classifier, quadratic classifier, K-nearest neighbor (KNN) algorithm [16] and Support Vector Machine (SVM). SVM were further examined by testing four different types of SVM classifiers and four different kernel functions. Regarding the type of SVM, C-Support Vector Classification (C-SVC), ν-Support Vector Classification (ν-SVC), ϵ-Support Vector Regression (ε-SVR) and ν-Support Vector Regression (ν-SVR) were examined [17]. Regarding the kernel function, we tested linear, polynomial, radial basis function and sigmoid function.

Classification was based on "Hold-out K-folds" cross-validation approach [18]. For this reason, the images of CBs and non-CBs were randomly divided K times (K=100) into training (60%) and testing (40%) set. During each repetition, all classifiers were applied on the same testing set. Average accuracy values were computed for each classifier over the K repetitions.

III. EXPERIMENTAL RESULTS

The methodology described in the previous section was applied on the CERTH/AUTH annotated database, containing 120 CB images and 180 non-CB images. Specifically, to generate the database, a set of nine ×400 microscopic images, derived from tissue biopsies of grade II and III FL, stained with H&E, were acquired at the Pathology Department of Medical School of Aristotle University of Thessaloniki, Greece. Tissue sections were sliced at a thickness of 1 to 1.5μm. They were scanned using Nikon DN100 digital network camera and were inspected by two medical experts, in order to identify the number of CBs in each image. By using these markings, a set of cropped images of 120 CB cells was created, containing only the nucleus of the cell and its neighborhood. The interior of the nucleus has been manually annotated in these images. Similarly, a second set of 180 cropped images containing only non-CBs was created. Non-CB cells were carefully selected in order to include a variety of cell types, ranging from small dark cells to large bright cells (like endothelial cells). In total, the generated dataset consists of 300 cell images and is available at [7].

TABLE I. EXPERIMENTAL RESULTS WITH DIFFERENT CLASSIFIERS

Classifier type	*Accuracy*	*Sensitivity*	*Specificity*
Classification Tree	95.42%	93.54%	96.67%
Naïve Bayes	90.29%	89.23%	91.00%
KNN	95.03%	95.5%	95.00%
Quadratic	94.2%	97.57%	91.93%
SVM (radial, ε-SVR)	97.44%	97.04%	97.73%

As described in the previous section, the dataset was randomly divided into 60% training and 40% testing sets 100 times and all classifiers were applied on the same testing set during each repetition. Average accuracy, specificity and sensitivity values are presented in Table I. All classifiers

yielded sufficiently good classification results, which confirm the descriptive ability of the selected feature set. Especially, SVM classification, using ε-SVR and radial basis kernel function, yielded the optimum results, with accuracy, sensitivity and specificity values of 97.44%, 97.04% and 97.73% respectively. A detailed analysis of features' performance is presented in Fig. 6. As it is clearly shown, all the features contribute significantly to the classification process. Especially, three of the proposed features, i.e. nuclear area, mean histogram value of the nucleus and the GLN seem to be the most discriminative features.

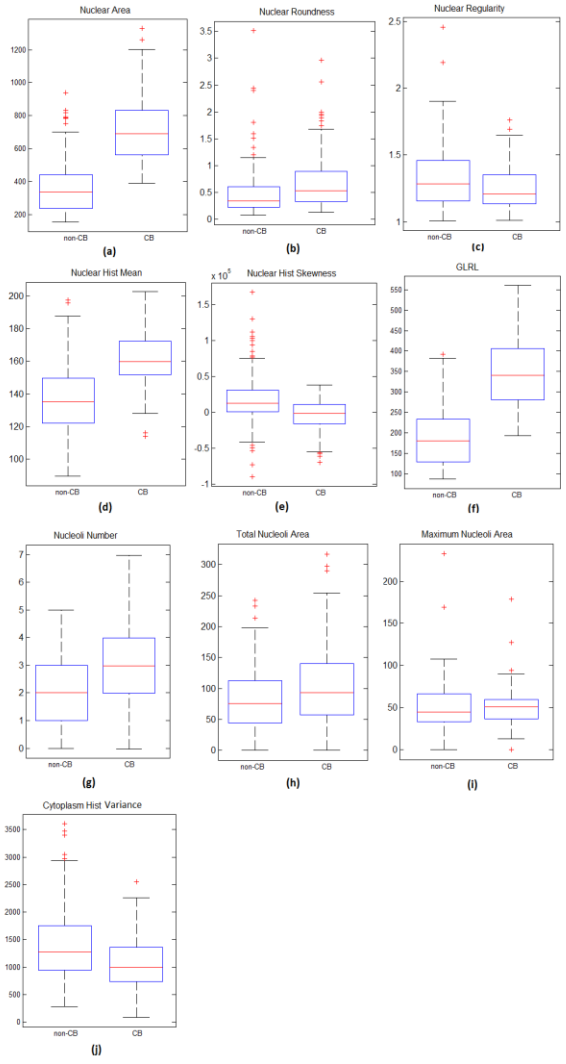

Figure 6. *Comparison of classification features between annotated CBs (right boxplots) and non-CBs (left boxplots). a) nuclear area, b) nuclear roundness, c) nuclear regularity (elipse residual), d) mean intensity histogram of the nucleus, e) skewness of intensity histogram of the nucleus, f) GLN, g) number of nucleoli, h) total nucleoli area, i) maximum nucleoli area, j) mean inensity histogram of the cytoplasm.*

IV. Conclusion

This paper presents a novel approach for discriminating centroblasts from non-centroblasts in H&E stained images of follicular lymphoma derived from tissue sections sliced at 1-1.5μm. More specifically, the method proposes a morphological and textural analysis for the extraction of a new set of features related to the nuclei, nucleoli and cytoplasm of the cells. Different types of classifiers were tested over an annotated dataset of cropped images of CBs and non-CBs derived from HPF images. Average accuracy results of 97.44% show the great potential of the proposed method. Future work will focus on a) the encapsulation of the proposed classification approach on a complete framework for automatic grading of FL images and b) the use of the proposed method in a variety of images with different concentrations of Hematoxylin and Eosin.

References

[1] A. Freedman, "Follicular Lymphoma: 2012 Update on Diagnosis and Management," *Am. J. Hematol*., vol. 87, no 10, pp. 988-995, Sep. 2012.

[2] O. Sertel, J. Kong, Ü. V. Çatalyürek, G. Lozanski, J. H. Saltz, and M. N. Gurcan, "Histopathological Image Analysis Using Model-Based Intermediate Representations and Color Texture: Follicular Lymphoma Grading," *Signal Processing Systems*, vol. 55, no. 1-3, pp 169-183, Apr. 2009.

[3] O. Seterl, G. Lozanski, A. Shana'ah, M. Gurcan, "Computer-Aided Detection of Centroblasts for Follicular Lymphoma Grading Using Adaptive Likelihood-Based Cell Segmentation," *IEEE Trans. Biomed. Eng*., vol. 57, no. 10, pp. 2613-2616, Oct. 2010.

[4] O. Sertel, G. Lozanski, A. Ahana'aah, and M. Gurcan, "Extraction of Color Features in the Spectral Domain to Recognize Centroblasts in Histopathology," in *Conf. Proc. IEEE Eng. Med. Biol. Soc*.; Minneapolis, USA, 2009, pp. 3685-3688.

[5] B. Oztan, H. Kong, M. Gurcan, and B. Yener, "Follicular Lympoma Grading using Cell-Graphs and Multi-Scale Feature Analysis," in *Proc. SPIE Medical Imaging*, San Diego, USA, 2012, pp. 831516-831516.

[6] E. N. Kornaropoulos, M. Niazi, G. Lozanski, and M. N. Gurcan, "Histopathological image analysis for centroblasts classification through dimensionality reduction approaches," *Cytometry Part A*, vol. 85, no. 3, pp. 245-255, Mar. 2014.

[7] CERTH/AUTH database available at: http://195.251.117.47 /miracle/fl_dataset

[8] E. S. Jaffe, N. L. Harris, J. Vardiman, E. Campo, and D. A. Arber, *Hematopathology 1st ed.*, Elsevier Health Sciences, Philadelphia, USA, 2010, pp. 267-290.

[9] M. J. Levesque, and R. M. Nerem, "The elongation and orientation of cultured endothelial cells in response to shear stress," *Journal of biomechanical engineering*, vol. 107 no. 4, pp. 341-347, Nov. 1985.

[10] W. Gander, G. H. Golub, and R. Strebel, "Least-square fitting of circles and ellipses," BIT, vol. 34, no. 4, pp. 558-578, Dec. 1994.

[11] M. M. Galloway, "Texture analysis using gray level run lengths," *Computer graphics and image processing*, vol. 4, no. 2, pp. 172-179, June 1975.

[12] X. Tang, "Texture information in run-length matrices," *IEEE Trans. Image Process.*, vol. 7, no. 11, pp. 1602-1609, Nov. 1998.

[13] J. Rissanen, "A Universal Prior for Integers and Estimation by Minimum Description Length," *Ann. Statist.*, vol. 11, no. 2, pp. 416-431, June 1983.

[14] H. K. Yuen, J. Princen, J. Illingworth, and J. Kittler, "Comparative study of Hough Transform methods for circle finding," *Image and Vision Computing*, vol. 8, no. 1, pp. 71–77, Feb. 1990.

[15] M. Grochtmann and K. Grimm, "Classification trees for partition testing," *Software Testing, Verification and Reliability*, vol. 3, no. 2, pp. 63-82, June 1993.

[16] N. S. Altman, "An introduction to kernel and nearest-neighbor nonparametric regression," *The American Statistician*, vol. 46, no. 3, pp. 175-185. Feb. 1992.

[17] C. C. Chang, and C. J. Lin, "LIBSVM: a library for support vector machines," *ACM Transactions on Intelligent Systems and Technology*, vol. 2 no. 3, 27, Apr. 2011.
S. Arlot, and A. Celisse, "A survey of cross-validation procedures for model selection," *Statistics Survey*, vol. 4, pp. 40-79, March 2010.